32. Two-dimensional generalized thermo-elastic problem for anisotropic half-space

Debkumar Ghosh[1], Abhijit Lahiri[2], Ibrahim A. Abbas[3]
[1, 2]Department of Mathematics, Jadavpur University, Kolkata, 700032, India
[3]Department of Mathematics, Sohag University, Sohag, Egypt
[1]Corresponding author
E-mail: [1]*debkumarghosh2020@gmail.com*, [2]*lahiriabhijit2000@yahoo.com*, [3]*ibrabbas7@yahoo.com*

Received 8 February 2017; accepted 12 March 2017
DOI https://doi.org/10.21595/mme.2017.18236

Check for updates

Abstract. This paper concerns with the study of wave propagation in fibre reinforced anisotropic half space under the influence of temperature and hydrostatic initial stress. Lord-Shulman theory is applied to the heat conduction equation. The resulting equations are written in the form of vector matrix differential equation by using Normal Mode technique, finally which is solved by Eigen value approach.

Keywords: eigenvalue, generalized thermoelasticity, normal mode, vector-matrix differential equation.

Nomenclature

u_i	Displacement tensor
t	Time variable
σ_{ij}	Stress components
ρ	Mass density
e_{ij}	Strain components
ω_{ij}	Rotational tensor
T	Temperature
T_0	Reference temperature
β_{ij}	Thermal elastic coupling tensor
c_e	Specific heat at constant strain
K_{ij}	Thermal conductivity
P	Initial pressure
t_0	Relaxation time
δ_{ij}	Kronecker Delta
λ, μ_T	Elastic parameters
$\alpha, \beta, (\mu_L - \mu_T)$	Reinforced elastic parameter

1. Introduction

Fibre-reinforced composite(FRC) materials are usually low weight and high strength used in construction engineering. The physical property of FRC material is governed by the theory of elasticity for different materials with the direction along the direction of fibre. Green [1] studied wave propagation in anisotropic elastic plates. Abbas and Othman [2] discussed the distribution of wave propagation under hydrostatic initial stress of fibre-reinforced materials in anisotropic half-space. Baylies and Green [3] analyse the flexural waves in fibre-reinforced laminated plates. Rogerson [4] discussed effect of penetration in a six-ply composite laminates.

Most of the thermoelasticity and generalized thermoelasticity (coupled or uncoupled) problems have been solved by potential function approach. This method is not always suitable as discussed by Dhaliwal and Sherief [5] and Sherief and Anwar [6]. These may be summarized by the initial conditions and the boundary conditions for physical problems which are directly concern with the material quantities under consideration and not with the potential function. Also, the potential function representations are not convergent always while the physical problems in

natural variables constitute convergent solution. So, the alternative method of potential function approach is eigenvalue approach. In this method, we obtain a vector-matrix differential equation from the basic equations which reduces finally to an algebraic eigenvalue problem and the solutions for the field variables are obtained by determining the eigenvalues and eigenvectors from the corresponding coefficient matrix. In this theory, body forces and/or heat sources are also accommodated as in Das and Lahiri [7], Bachher et al. [8]. Now, two different models of generalized thermoelastisities are extensively used. One is Lord and Shulman (L-S) [9] theory and the other is Green and Lindsay (G-L) [10] theory. Introducing one relaxtion time parameter in L-S theory the heat conduction equation becomes hyperbolic type without violating conventional Fourier's law. Whereas the G-L theory modified the heat conduction equation as well as the equation of motion in coupled thermoelasticitywo relaxation time parameters. There are other three models (Model I, II and III by Green and Nagdhi [11-13]) for generalized thermoelasticity concerned to the theory of with or without energy dissipation.

2. Development of governing equations

The stress-strain relation and the governing equations of motion without body forces and heat sources are written as follow:

$$\sigma_{ij,j} - P\omega_{ij,j} = \rho\ddot{u}_i, \tag{1}$$

$$\sigma_{ij} = \lambda e_{kk}\delta_{ij} + 2\mu_T e_{ij} + \alpha\left(a_k a_m e_{km}\delta_{ij} + a_i a_j e_{kk}\right) + 2(\mu_L - \mu_T)\left(a_i a_k e_{kj} + a_j a_k e_{ki}\right) + \beta a_k a_m e_{km} a_i a_j - \beta_{ij}(T - T_0)\delta_{ij}, \quad i,j,k,m = 1,2,3, \tag{2}$$

$$e_{ij} = \frac{1}{2}\left(u_{i,j} + u_{j,i}\right), \tag{3}$$

$$\omega_{ij} = \frac{1}{2}\left(u_{j,i} - u_{i,j}\right), \tag{4}$$

$$K_{ij}T_{ij} = \rho c_e\left(\dot{T} + t_0\ddot{T}\right) + T_0\left(\dot{u}_{i,j}\ddot{u}_{i,j}\right), \quad i,j = 1,2,3. \tag{5}$$

We consider the problem of a elastic half-space ($x \geq 0$) in fibre-reinforced anisotropic material with $a \equiv (a_1, a_2, a_3)$ where $a_1^2 + a_2^2 + a_3^2 = 1$ as in I. A. Abbas [14], where the displacements are given:

$$u = u_x = u(x,y,t), \quad v = u_y = v(x,y,t), \quad w = u_z = 0. \tag{6}$$

We consider the direction of fibre as $a \equiv (1,0,0)$ with x-axis as prefered direction, and Eqs. (1-5), reduces as given:

$$\sigma_{11} = (\lambda + 2\alpha + 4\mu_L - 2\mu_T + \beta)\frac{\partial u}{\partial x} + (\lambda + \alpha)\frac{\partial v}{\partial y} - \beta_{11}(T - T_0), \tag{7}$$

$$\sigma_{22} = (\lambda + 2\mu_T)\frac{\partial v}{\partial y} + (\alpha + \lambda)\frac{\partial u}{\partial x} - \beta_{22}(T - T_0), \tag{8}$$

$$\sigma_{12} = \mu_L\left(\frac{\partial v}{\partial x} + \frac{\partial u}{\partial y}\right), \tag{9}$$

$$A_{11}\frac{\partial^2 u}{\partial x^2} + \left(A_{12} + \mu_L - \frac{P}{2}\right)\frac{\partial^2 v}{\partial x \partial y} + \left(\mu_L + \frac{P}{2}\right)\frac{\partial^2 u}{\partial y^2} - \beta_{11}\frac{\partial T}{\partial x} = \rho\frac{\partial^2 u}{\partial t^2}, \tag{10}$$

$$A_{22}\frac{\partial^2 v}{\partial y^2} + \left(A_{12} + \mu_L - \frac{P}{2}\right)\frac{\partial^2 u}{\partial x \partial y} + \left(\mu_L + \frac{P}{2}\right)\frac{\partial^2 v}{\partial x^2} - \beta_{22}\frac{\partial T}{\partial y} = \rho\frac{\partial^2 v}{\partial t^2}, \tag{11}$$

$$K_{11}\frac{\partial^2 T}{\partial x^2} + K_{22}\frac{\partial^2 T}{\partial y^2} = \left(\frac{\partial}{\partial t} + t_0\frac{\partial^2}{\partial t^2}\right)\left(\rho c_e T + T_0\beta_{11}\frac{\partial u}{\partial x} + T_0\beta_{22}\frac{\partial v}{\partial y}\right), \tag{12}$$

with:

$$A_{11} = \lambda + 2(\alpha + \mu_L) + 4(\mu_L - \mu_T) + \beta, \quad A_{12} = \alpha + \lambda, \quad A_{22} = \lambda + 2\mu_T,$$
$$\beta_{11} = (2\lambda + 3\alpha + 4\mu_L - 2\mu_T + \beta)\alpha_{11} + (\lambda + \alpha)\alpha_{22}, \quad \beta_{22} = (2\lambda + \alpha)\alpha_{11} + (\lambda + 2\mu_T)\alpha_{22},$$

where α_{11}, α_{22} are linear thermal expansion coeeficients.

To transform the above governing equations in non-dimensional forms, we introduce the non-dimensional variables as follows:

$$(x', y', u', v') = c_1\chi(x, y, u, v), \quad t' = c_1^2\chi t, \quad T' = \frac{\beta_{11}(T - T_0)}{\rho c_1{}^2}, \quad \chi = \frac{\rho c_e}{K_{11}},$$
$$(\sigma'_{11}, \sigma'_{12}, \sigma'_{22}) = \frac{1}{\rho c_1^2}(\sigma_{11}, \sigma_{12}, \sigma_{22}), \quad c_1^2 = \frac{A_{11}}{\rho}. \tag{13}$$

Using non-dimensional Eq. (13), the governing equations reduces to (eleminating primes for convenience):

$$\sigma_{11} = \frac{\partial u}{\partial x} + B_1\frac{\partial v}{\partial y} - T, \tag{14}$$

$$\sigma_{22} = B_1\frac{\partial u}{\partial x} + B_2\frac{\partial v}{\partial y} - B_3 T, \tag{15}$$

$$\sigma_{12} = B_4\left(\frac{\partial v}{\partial x} + \frac{\partial u}{\partial y}\right), \tag{16}$$

$$\frac{\partial^2 u}{\partial x^2} + \left(B_1 + B_4 - \frac{R_p}{2}\right)\frac{\partial^2 v}{\partial x \partial y} + \left(B_4 + \frac{R_p}{2}\right)\frac{\partial^2 u}{\partial y^2} - \frac{\partial T}{\partial x} = \frac{\partial^2 u}{\partial t^2}, \tag{17}$$

$$B_2\frac{\partial^2 v}{\partial y^2} + \left(B_1 + B_4 - \frac{R_p}{2}\right)\frac{\partial^2 u}{\partial x \partial y} + \left(B_4 + \frac{R_p}{2}\right)\frac{\partial^2 v}{\partial x^2} - B_3\frac{\partial T}{\partial y} = \frac{\partial^2 v}{\partial t^2}, \tag{18}$$

$$\frac{\partial^2 T}{\partial x^2} + \varepsilon_1\frac{\partial^2 T}{\partial y^2} = \left(\frac{\partial}{\partial t} + t_0\frac{\partial^2}{\partial t^2}\right)\left(T + \varepsilon_2\frac{\partial u}{\partial x} + \varepsilon_3\frac{\partial v}{\partial y}\right), \tag{19}$$

where:

$$(B_1, B_2, B_3) = \frac{1}{A_{11}}(A_{12}, A_{22}, \mu_1), \quad B_3 = \frac{\beta_{22}}{\beta_{11}}, \quad R_p = \frac{P}{A_{11}},$$
$$(\varepsilon_2, \varepsilon_3) = \frac{T_0\beta_{11}}{A_{11}\rho c_e}(\beta_{11}, \beta_{22}), \quad \varepsilon_1 = \frac{K_{11}}{K_{22}}.$$

3. Solution procedure

3.1. Normal mode analysis: formulation of vector-matrix differential equation

For the solution of the Eqs. (14-19), physical variables can be decomposed using normal modes Eq. (20) in the following form:

$$[u, v, T, \sigma_{11}, \sigma_{12}, \sigma_{22}](x, y, t) = [u^*, v^*, T^*, \sigma_{11}^*, \sigma_{12}^*, \sigma_{22}^*](x)e^{\omega t + iay}, \tag{20}$$

where $i = \sqrt{-1}$, ω is the angular frequency and a is the wave number along x-axis.

Using Eq. (20), Eqs. (14-19) reduces to omitting '*' for convenience:

$$\sigma_{11} = \frac{du}{dx} + (B_1 ia)v - T, \tag{21}$$

$$\sigma_{22} = B_1 \frac{du}{dx} + (B_2 ia)v - B_3 T, \tag{22}$$

$$\sigma_{12} = B_4 \frac{dv}{dx} + (B_4 ia)u, \tag{23}$$

$$\frac{d^2u}{dx^2} = M41.u + 0.v + 0.T + 0.u' + M45.v' + T', \tag{24}$$

$$\frac{d^2v}{dx^2} = 0.u + M52.v + M53.T + M54.u' + 0.v' + 0.T', \tag{25}$$

$$\frac{d^2T}{dx^2} = 0.u + M62.v + M63.T + M64.u' + 0.v' + 0.T', \tag{26}$$

where:

$$M41 = a^2\left[B_4 + \frac{R_p}{2}\right] + \omega^2, \quad M45 = -ia\left[B_1 + B_4 - \frac{R_p}{2}\right], \quad M52 = \frac{a^2 B_2 + \omega^2}{B_4 + \frac{R_p}{2}},$$

$$M53 = \frac{\frac{R_p}{2} - B_1 - B_4}{B_4 + \frac{R_p}{2}}, \quad M54 = \frac{iaB_3}{B_4 + \frac{R_p}{2}}, \quad M62 = ia\varepsilon_3(\omega + t_0\omega^2),$$

$$M63 = \omega + t_0\omega^2 + \varepsilon_2 a^2, \quad M64 = \varepsilon_2^2(\omega + t_0\omega^2).$$

Eqs. (24-26) can be written in the form of vector-matrix differential equation as [2, 8]:

$$\frac{d\vec{W}}{dx} = \vec{A}\vec{W}, \tag{27}$$

where $\vec{W}$ =[u v T u' v' T']^T and $A = \begin{bmatrix} L_{11} & L_{12} \\ L_{21} & L_{22} \end{bmatrix}$. Where L_{11} is null matrix and L_{12} identity matrix of order 3×3 respectively and L_{21} and L_{22} are given by:

$$L_{11} = \begin{pmatrix} 0 & 0 & 0 \\ 0 & 0 & 0 \\ 0 & 0 & 0 \end{pmatrix}, \quad L_{12} = \begin{pmatrix} 1 & 0 & 0 \\ 0 & 1 & 0 \\ 0 & 0 & 1 \end{pmatrix},$$

$$L_{21} = \begin{pmatrix} M41 & 0 & 0 \\ 0 & M52 & M53 \\ 0 & M62 & M63 \end{pmatrix}, \quad L_{22} = \begin{pmatrix} 0 & M45 & 1 \\ M54 & 0 & 0 \\ M64 & 0 & 0 \end{pmatrix}.$$

3.2. Solution of the vector-matrix differential equation

To solve the vector-matrix differential Eq. (27), we apply the method of eigenvalue approach, The characteristic equation of the matrix $\vec{A}$ is given by:

$$|A - \lambda I| = 0. \tag{28}$$

The roots of the characteristic Eq. (28) are $\lambda = \lambda_i$, $i = 1, 2, 3$ which are of the form $\lambda = \pm\lambda_1$, $\lambda = \pm\lambda_2$ and $\lambda = \pm\lambda_3$ and they are also eigenvalues of the matrix.

The eigenvector, $\vec{W}$ corresponding to the eigenvalue λ can obtained as:

$$\vec{X}_\lambda = [\delta_1 \quad \delta_2 \quad \delta_3 \quad \lambda\delta_1 \quad \lambda\delta_2 \quad \lambda\delta_3]^T, \tag{29}$$

where $\delta_1 = a_2b_3 - a_3b_2$, $\delta_2 = a_3b_1 - a_1b_3$, $\delta_3 = a_1b_2 - a_2b_1$.

As in Lahiri et al. [7], the general solution of Eq. (27) which is regular as can be written as:

$$\overrightarrow{W} = \sum_{i=1}^{3} A_i X_i e^{-\lambda_i x}, \quad x \geq 0. \tag{30}$$

Hence the field variables can be written as the following:

$$u = A_1x_{11}e^{-\lambda_1 x} + A_2x_{21}e^{-\lambda_2 x} + A_3x_{31}e^{-\lambda_3 x},$$
$$v = A_1x_{12}e^{-\lambda_1 x} + A_2x_{22}e^{-\lambda_2 x} + A_3x_{32}e^{-\lambda_3 x},$$
$$T = A_1x_{13}e^{-\lambda_1 x} + A_2x_{23}e^{-\lambda_2 x} + A_3x_{33}e^{-\lambda_3 x}.$$

The simplified form of Eqs. (21-23) can be written as:

$$\sigma_{11} = A_1R_{11}(x) + A_2R_{12}(x) + A_3R_{13}(x),$$
$$\sigma_{22} = A_1R_{21}(x) + A_2R_{22}(x) + A_3R_{23}(x),$$
$$\sigma_{33} = A_1R_{31}(x) + A_2R_{32}(x) + A_3R_{33}(x),$$

where:

$$R_{11}(x) = [-\lambda_1x_{11} + B_1iax_{12} - x_{13}]e^{-\lambda_1 x},$$
$$R_{12}(x) = [-\lambda_2x_{21} + B_1iax_{22} - x_{23}]e^{-\lambda_2 x},$$
$$R_{13}(x) = [-\lambda_3x_{31} + B_1iax_{32} - x_{33}]e^{-\lambda_3 x},$$
$$R_{21}(x) = [-\lambda_1B_1x_{11} + B_2iax_{12} - B_3x_{13}]e^{-\lambda_1 x},$$
$$R_{21}(x) = [-\lambda_2B_1x_{21} + B_2iax_{22} - B_3x_{23}]e^{-\lambda_2 x},$$
$$R_{21}(x) = [-\lambda_3B_1x_{31} + B_2iax_{32} - B_3x_{33}]e^{-\lambda_3 x},$$
$$R_{31}(x) = [B_4iax_{11} - \lambda_1x_{12}]e^{-\lambda_1 x},$$
$$R_{32}(x) = [B_4iax_{21} - \lambda_2x_{22}]e^{-\lambda_2 x},$$
$$R_{33}(x) = [B_4iax_{31} - \lambda_3x_{32}]e^{-\lambda_3 x}.$$

4. Boundary conditions

Considering the problem of a half-space ϕ, defined as follows:

$$\phi = (x, y, z): 0 \leq x \leq \infty, \quad -\infty \leq y \leq \infty, \quad -\infty \leq z \leq \infty.$$

In order to determine the arbitrary constants $A_i's$, $i = 1, 2, 3$, we consider the boundary conditions as follows.

4.1. Case 1

a) Mechanical Boundary condition:
For stress-free surface x =0, $\sigma_{11} = 0$, $\sigma_{12} = 0$.
b) Thermal Boundary condition:

$$\nu T - \frac{dT}{dx} = r, \tag{31}$$

where ν is Biot's number.

4.2. Case 2

a) Mechanical Boundary condition:
For stress-free surface $x = 0$, $\sigma_{11} = -P_1 + P_2 e^{\omega t + iay}$, $\sigma_{12} = 0$.
b) Thermal Boundary condition:

$$T = P_3 e^{\omega t + iay}. \tag{32}$$

5. Numerical analysis

5.1. Case 1

5.1.1. Distribution of different stress components

Fig. 1 represents distribution of normal stress σ_{11} for $y = 0.3$.
For fixed time t, σ_{11} gradually increases as x increases. For fixed x numerical values of σ_{11} gradually decreases as t increases.
Fig. 2 represents distribution of normal stress σ_{12} for $y = 0.2$.
For fixed time t, σ_{12} gradually decreases as x increases. For fixed x numerical values of σ_{12} gradually increases as t increases.
Fig. 3 represents distribution of normal stress σ_{22} for $y = 0.5$.
For fixed time t, σ_{22} gradually decreases as x increases. For fixed x numerical values of σ_{12} gradually increases as t increases.

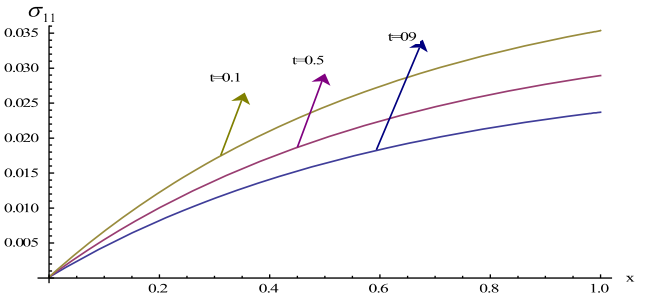

Fig. 1. Stress component σ_{11} at $y = 0.3$ for different values of t verses x

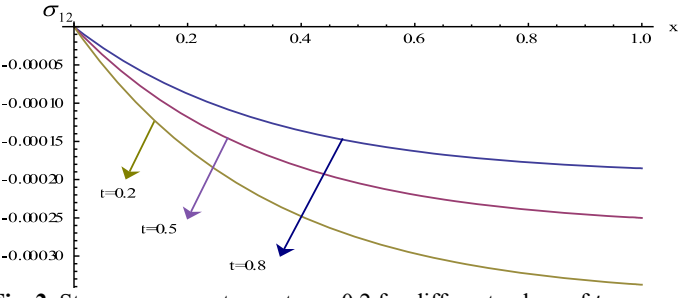

Fig. 2. Stress component σ_{12} at $y = 0.2$ for different values of t verses x

Fig. 4 represents distribution of normal stress σ_{11} for different values of x and y for fixed $t = 0.1$ and $\omega = 0.5$.
x numerical value of σ_{11} gradually decreases as y increases. For fixed y the numerical value of σ_{11} gradually increases as x increases. σ_{11} is maximum when $x = 1$ and $y = 0$.
Fig. 5 represent distribution of normal stress σ_{12} for different values of x and y for fixed $t = 0.4$ and $\omega = 5$.

For fixed x numerical value of σ_{12} gradually decreases as y increases. For fixed y the numerical value of σ_{12} gradually decreases as x increases. Significant changes occur in the region $0.2 \leq x \leq 0.6$ and $0.6 \leq y \leq 1.0$.

Fig. 6 represent distribution of stress component σ_{22} at for different values of x and y for fixed $t = 0.1$ and 0.1.

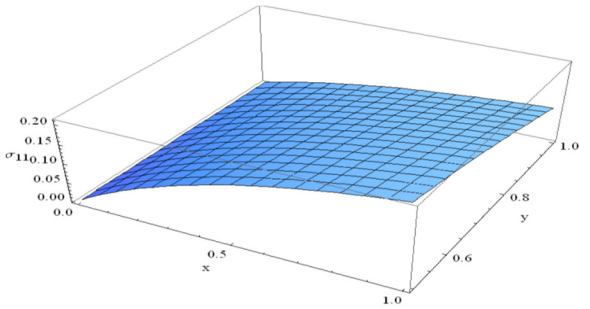

Fig. 4. Stress component σ_{11} at $t = 0.1$ and $\omega = 0.5$ verses x and y

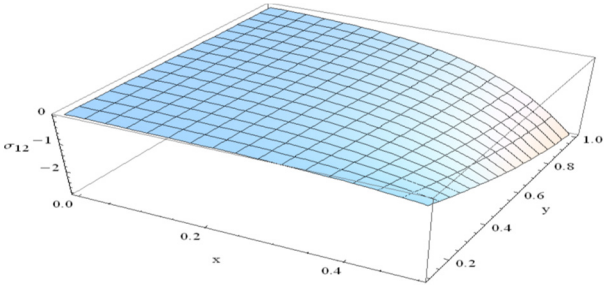

Fig. 5. The variation of stress component σ_{12} at $t = 0.4$ and $\omega = 3$ verses x and y

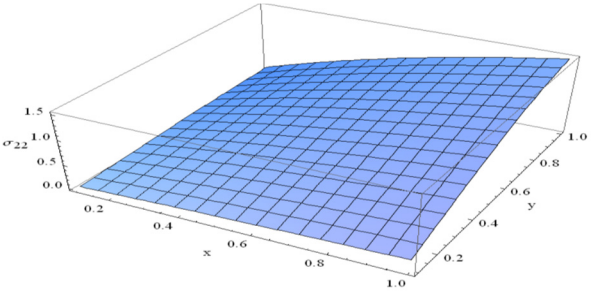

Fig. 6. Stress component σ_{22} at $t = 0.1$ and $\omega = 0.1$ verses x and y

For fixed x numerical value of σ_{22} gradually increases as y increases. For fixed y numerical value of σ_{22} gradually increases as x increases.

Fig. 7 represent distribution of normal stress σ_{12} for different values of x and t for fixed $y = 0.2$ and 1.

For fixed x, nominal decreasing of numerical values of σ_{12} has been seen as t increases, while For fixed t, numerical values of σ_{12} decreases gradually as x increases. numerical values of σ_{12} minimum at $x = 1$ and $0.02 \leq t \leq 0.1$

Fig. 8 represent distribution of normal stress σ_{22} for different values of x and t for fixed $y = 0.5$ and 2.

For fixed x, nominal decreasing of σ_{22} has been seen as t increases. For fixed t, numerical values of σ_{12} decreases as x increases. Also, significant changes occur in the region $0.6 \leq x \leq 1.0$ and $0 \leq t \leq 1.0$.

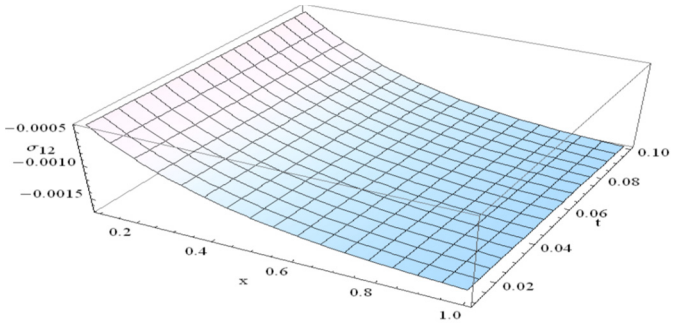

Fig. 7. Stress component σ_{12} at $y = 0.2$ and $\omega = 1$ verses x and t

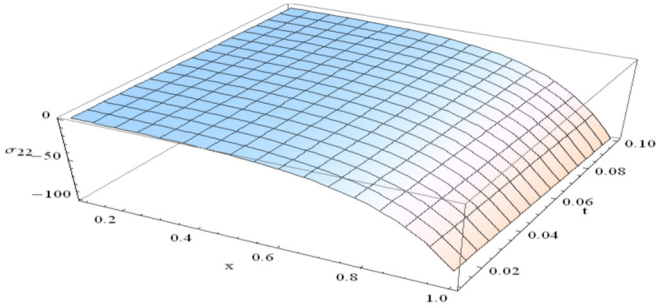

Fig. 8. The distribution of stress component σ_{22} at $y = 0.5$ and $\omega = 2$ verses x and t

5.1.2. Distribution of temperature

Fig. 9 represent distribution of temperature, T for different values of x and y for fixed $t = 0.3$ and 2.

For fixed x numerical value of T gradually decreases as y increases. For fixed y numerical value of T gradually increases as x increases. T in minimum at $x = 0$ and significant changes occurs in the region $0.6 \leq x \leq 1.0$ and $0 \leq y \leq 1.0$

Fig. 10 represent distribution of temperature, T for different values of x and t for fixed $y = 0.1$ and 1.5.

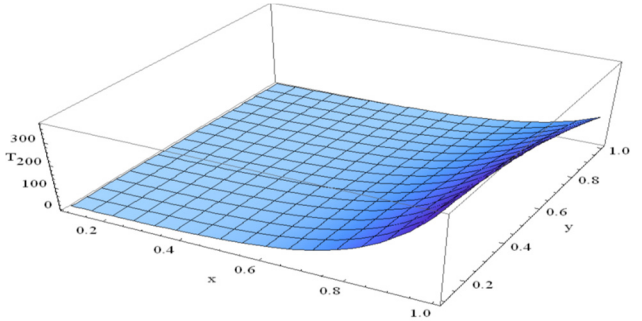

Fig. 9. The variation of T at $t = 0.3$ and $\omega = 2$ verses x and y

For fixed t numerical value of T nominally increases as x increases. For fixed x numerical value of T gradually increases as t increases.

Fig. 11 represent distribution of temperature, T for different values of y and t for fixed $x = 0.5$ and 3.

For fixed t numerical value of T nominally increases as y increases. For fixed x numerical values of T decreases as t increases.

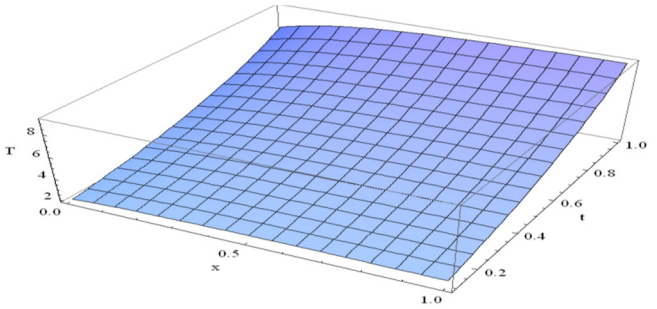

Fig. 10. Variation of T at $y = 0.1$ and $\omega = 1.5$ verses x and t

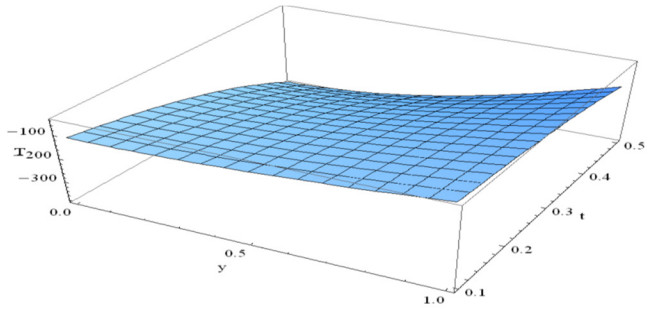

Fig. 11. Variation of T at $x = 0.5$ and $\omega = 3$ verses y and t

5.2. Case 2

5.2.1. Distribution of different stress components

Fig. 12 represents distribution of normal stress σ_{11} for $y = 0.3$, $t = 0.01$ and 5 for different numerical values of R_p.

For fixed R_p, σ_{11} gradually decreases as x increases. For fixed x numerical values of σ_{11} gradually decreases as R_p increases.

Fig. 13 represents distribution of normal stress σ_{11} for $y = 0.3$, $t = 0.01$ and 5 for different fractional values of R_p.

For fixed time R_p, σ_{11} gradually increases as x increases. For fixed x numerical values of σ_{11} gradually decreases as R_p increases. Significant changes occurred for $0 \leq x \leq 0.4$.

Fig. 14 represents the distribution of stress component σ_{12} at $y = 0.2$, $t = 0.03$ and 0.3 for different fractional values R_p of verses x for $P1 = 1$.

For fixed time R_p, σ_{11} gradually decreases as x increases. For fixed x numerical values of σ_{11} increases as R_p increases. Significant changes occurred for $0 \leq x \leq 0.4$.

Fig. 15 represents the distribution of stress component σ_{12} at $y = 0.3$, $t = 0.1$ and 4 for different integral values R_p for $P1 = 0$.

For fixed Rp, σ_{12} gradually decreases as x increases. For fixed x numerical values of σ_{12} increases as R_p increases.

Fig. 16 represents the distribution of stress component σ_{22} at $y = 0.2$, $t = 0.6$ and 0.4 for different values R_p for $P1 = 0$.

For fixed $R_p = 0.9$, σ_{22} gradually increases as x increases but for other fixed values of R_p, σ_{22} gradually decreases as x increases. For fixed x, σ_{22} gradually increases as x increases for $R_p = 0.9$ but for other fixed values of R_p, σ_{22} gradually decreases as x increases.

Fig. 17 represents the distribution of stress component σ_{11} for different values of t for fixed $y = 0.2$ and 1.5.

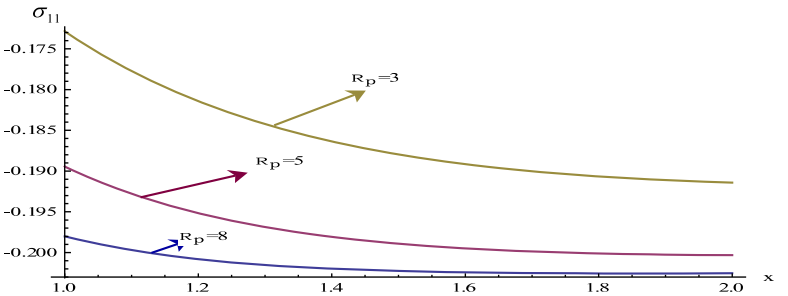

Fig. 12. Stress component σ_{11} at $y = 0.3$, $t = 0.01$ and $\omega = 5$ for different values R_p of verses x

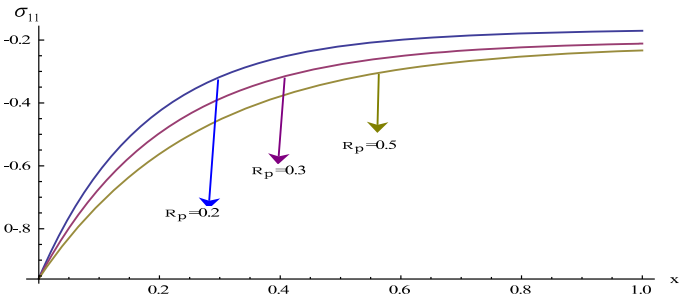

Fig. 13. Stress component σ_{11} at $y = 0.2$ and $\omega = 0.2$ for different values R_p of verses x

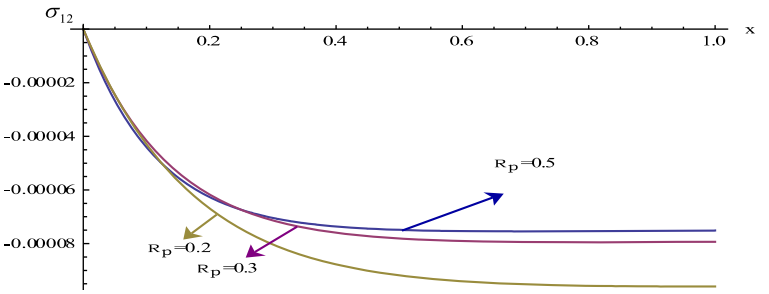

Fig. 14. Stress component σ_{12} at $y = 0.2$, $t = 0.03$ and $\omega = 0.3$ for different values R_p of verses x for $P1 = 1$

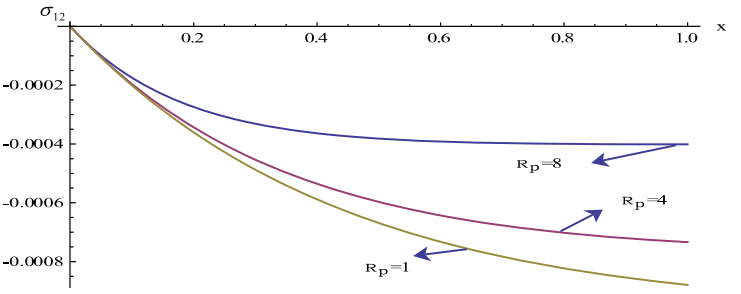

Fig. 15. Stress component σ_{12} at $y = 0.3$, $t = 0.1$ and $\omega = 4$ for different values R_p of verses x for $P1 = 0$

For fixed t, the numerical value of σ_{11} gradually increases as x increases. For fixed x, the numerical value of σ_{11} gradually increases as t increases.

Fig. 18 The distribution of stress component σ_{12} for fixed $y = 0.3$ and 0.5 for different values of t.

For fixed t, the numerical value of σ_{12} gradually decreases as x increases. For fixed x, the numerical value of σ_{12} gradually increases as t increases.

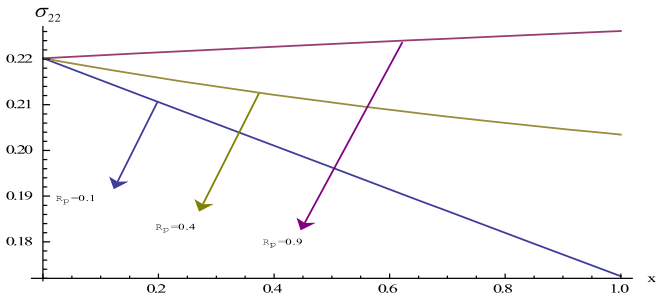

Fig. 16. Stress component σ_{22} at $y = 0.2$, $t = 0.6$ and $\omega = 0.4$ for different values R_p of verses x for $P1 = 0$

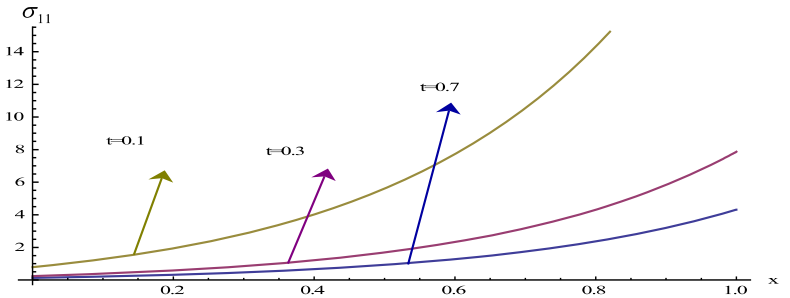

Fig. 17. Stress component σ_{11} at $y = 0.2$ and $\omega = 1.5$ for different values of t verses x

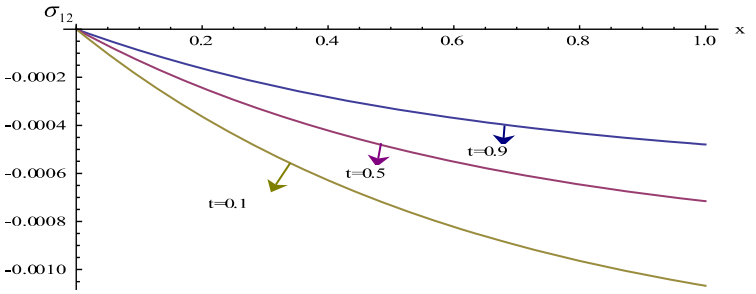

Fig. 18. Stress component σ_{12} at $y = 0.3$ and $\omega = 0.5$ for different values of t verses x

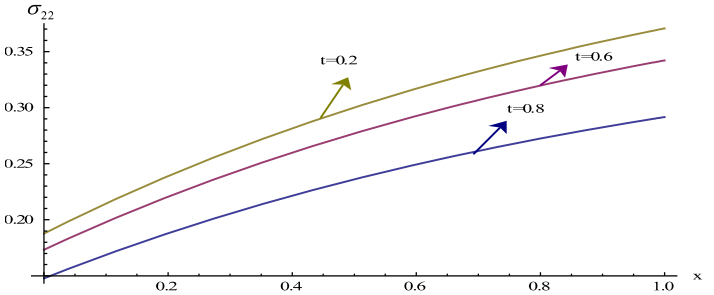

Fig. 19. Stress component σ_{22} at $y = 0.5$ and $\omega = 0.2$ for different values of t verses x

Fig. 19 represents the distribution of stress component σ_{22} at fixed $y = 0.5$ and 0.2 for different values of t.

For fixed t, the numerical value of σ_{12} gradually increases as x increases, but for fixed x, the numerical value of σ_{12} gradually decreases as t increases.

Fig. 20 represents distribution of normal stress σ_{11} for different values of x and for fixed

$t = 0.3$ and $y = 0.3$.

For fixed x numerical value of σ_{11} remain constant as increases, but for fixed ω the numerical value of σ_{11} gradually decreases as x increases.

Fig. 21 represents distribution of normal stress σ_{12} for different values of x and for fixed $y = 0.3$ and $t = 0.5$.

For fixed x, nominal increasing of numerical values of σ_{12} has been seen as increases, while for fixed ω, numerical values of σ_{12} increases gradually as x increases after $x = 0.6$ (approx.). Numerical values of σ_{12} minimum at $x = 0.5$ (approx.) and $1 \leq t \leq 3$.

Fig. 22 represents distribution of stress component σ_{22} at for different values of x and for fixed $t = 0.1$ and $y = 0.4$.

For fixed ω numerical value of σ_{22} gradually decreases as x increases. Numerical values of σ_{22} minimum at $x = 1$ and $0 \leq \omega \leq 1$.

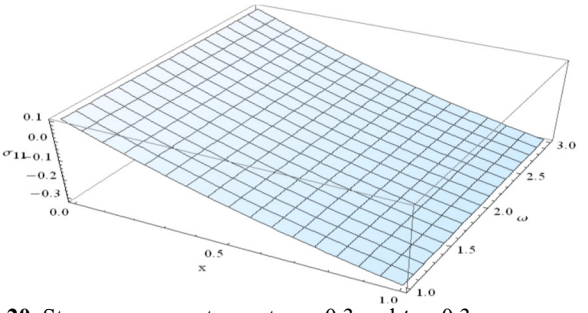

Fig. 20. Stress component σ_{11} at $y = 0.3$ and $t = 0.3$ verses x and ω

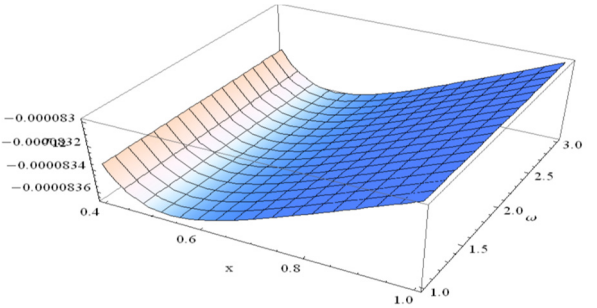

Fig. 21. Stress component σ_{12} at $y = 0.3$ and $t = 0.5$ verses x and ω

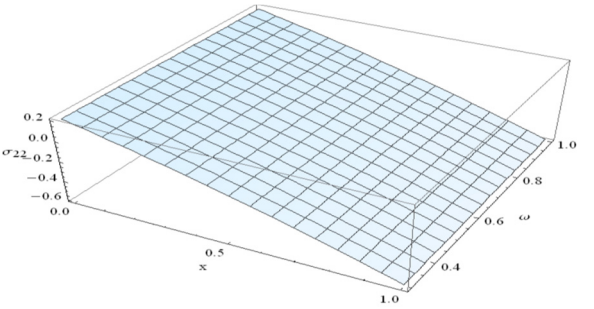

Fig. 22. Stress component σ_{22} at $y = 0.4$ and $t = 0.1$ verses x and ω

5.2.2. Distribution of temperature

Fig. 23 represents distribution of temperature, T for different values of x and ω for fixed $t = 0.1$ and $y = 0.4$.

For fixed x numerical value of T gradually increases in the region $0 \leq \omega \leq 0.3$ (approx.) For fixed ω numerical value of T nominally increases as x increases.

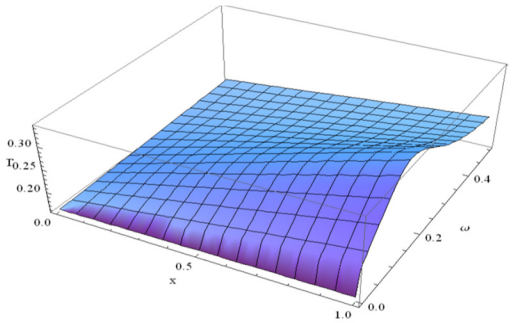

Fig. 23. The variation of T at y =0.4 and t = 0.1 verses x and ω

6. Conclusion

We consider the physical parameters in SI units given in Dhaliwal and Singh following below to obtain the numerical result to observe the effect of wave propagation:

$\rho = 2660kg/m^3,\ \lambda = 5.65\times10^{10}N/m^2,$
$\mu_T = 2.46\times10^{10}N/m^2,\ \mu_L = 5.66\times10^{10}N/m^2,$
$\alpha = -1.28\times10^{10}N/m^2,\ \beta = 220.90\times10^{10}N/m^2,$
$\alpha_{11} = 0.017\times10^{-4}deg^{-1},\ \alpha_{22} = 0.015\times10^{-4}deg^{-1},$
$l = 0.5,\ T_0 = 293K,\ c_e = 0.787\times10^3JKg^{-1}deg^{-1}$
$K_{11} = 0.0921\times10^{10}Jm^{-1}s^{-1}deg^{-1}$
$K_{22} = 0.0963\times10^{10}Jm^{-1}s^{-1}deg^{-1}$
$P_1 = 0\ or\ 1,\ P_2 = 0.1,\ P_3 = 0.2.$

References

[1] **Green W. A.** Bending waves in strongly anisotropic plates. Quarterly Journal of Mechanics and Applied Mathematics, Vol. 35, 1982, p. 485-507.

[2] **Abbas I. A., Othman M. I. A.** Generalized thermoelastic interaction in a fiber-reinforced anisotropic half-space under hydrostatic initial stress. Journal of Vibration Control, Vol. 18, Issue 2, 2011, p. 175-182.

[3] **Baylis E. R., Green W. A.** Flexural waves in fiber reinforced laminated plates. Journal of Sound and Vibration, Vol. 110, 1986, p. 1-26.

[4] **Rogerson G. A.** Penetration of impact waves in a six-ply fiber composite laminate. Journal of Sound and Vibration, Vol. 158, 1992, p. 105-120.

[5] **Dhaliwal R. S., Sherief H. H.** Generalized thermoelasticity for anisotropic media. Quarterly of Applied Mathematics, Vol. 33, 1980, p. 1-8.

[6] **Sherief H. H., El-Sayed A., El-Latief A.** Fractional order theory of thermoelasticity. International Journal of Solids and Structures, Vol. 47, 2010, p. 269-275.

[7] **Santra S., Das N. C., Kumar R., Lahir A.** Three dimensional fractional order generalized thermoelastic problem under effect of rotation in a half space. Journal of Thermal Stresses, Vol. 38, 2015, p. 309-324.

[8] **Bachher M., Sarkar N., Lahiri A.** Generalized thermoelastic infinite medium with voids subjected to a instantaneous heat sources with fractional derivative heat transfer. International Journal of Mechanical Sciences, Vol. 89, 2014, p. 84-91.

[9] **Lord H. W., Shulman Y.** A generalized dynamical theory of thermoelasticity. Journal of the Mechanics and Physics of Solids, Vol. 15, 1967, p. 299-309.

[10] **Green A. E., Lindsay K. A.** Thermoelasticity. Journal of Elasticity, Vol. 2, 1972, p. 1-7.

[11] **Green A. E., Naghdi P. M.** A re-examination of the basic results of thermomechanics. Proceedings of the Royal Society of London A, Vol. 432, 1991, p. 171-194.

[12] **Green A. E., Naghdi P. M.** On undamped heat waves in an elastic solid. Thermal Stresses, Vol. 15, 1992, p. 252-264.

[13] **Green A. E., Naghdi P. M.** Thermoelasticity without energy dissipation. Elasticity, Vol. 31, 1993, p. 189-208.

[14] **Ibrahim A. Abbas** Generalized magnetothermoelasticity in a fiber-reinforced anisotropic half-space. International Journal of Thermophysics, 2011, https://doi.org/10.1007/s10765-011-0957-3.